Materials and Structures (2006)
DOI 10.1617/s11527-005-9037-0

Influence of microstructure on the resistance to salt crystallisation damage in brick

D. Benavente · L. Linares-Fernández · G. Cultrone · E. Sebastián

Received: 15 November 2004 / Accepted: 28 February 2005

Abstract In the article we study the variation of brick durability and, more specifically, its resistance to salt crystallisation produced by changes in its microstructure during firing. For this purpose, the evolution of both mechanical and pore structure properties are studied within a wide range of temperatures (700–1100°C). An increase in the firing temperature produces a more homogeneous and resistant brick, measured using ultrasound velocity and uniaxial compressive strength. This result is obtained thanks to the vitrification process and changes in the brick's pore structure: larger, rounder pores, which are quantified by their roundness and fractal dimension. As a result of these changes, an excellent durability is achieved in the bricks studied when fired at temperatures above 1000°C. Considering that few differences are noted in pore structure and brick strength between 1000 and 1100°C, the recommended firing temperature is, for raw materials with a similar composition and production process, 1000°C, as this involves a lower production cost than firing at 1100°C.

Résumé *Cet article étudie la variation de la durabilité de la brique et, plus précisément, sa résistance à la cristallisation du sel due aux modifications de sa microstructure lors de la cuisson. A cet effet, l'évolution des propriétés mécaniques et de la structure des pores est étudiée sur une large gamme de températures (700–1100°C). Une augmentation de la température de cuisson qui donne une brique plus résistante et homogène est mesurée par vélocimétrie ultrasonore et résistance à la compression uniaxiale. Ce résultat est obtenu grâce au processus de vitrification et à des modifications de la structure des pores: des pores plus grands et plus ronds qui sont quantifiés par leur rondeur et leur dimension fractale. Ces modifications offrent aux briques étudiées une excellente durabilité lorsqu'elles sont cuites à des températures supérieures à 1000°C. Etant donné qu'à peine quelques différences ont été détectées dans la structure des pores et dans la résistance de la brique entre 1000 et 1100°C, la température de cuisson recommandée est de 1000°C, pour les matières premières composées et fabriquées de la même manière, car le matériau produit à cette température implique des coûts plus bas que s'il est cuit à 1.100°C.*

1. Introduction

Brick is a building material whose durability may be reduced when subjected to deterioration processes. In particular, the crystallisation pressure of soluble salts is one of the most important decay processes that affect the durability of these porous materials. The incidence of salt crystallisation depends on the pore structure, the saturation degree of the salt and the magnitude of the repelling force between the salt and the confining pore surface [1, 2].

Moreover, salt damage depends on the environment in which precipitation occurs. Salt decay mainly occurs when salt crystallisation is produced at a certain distance beneath the external surface. This kind of crystallisation forms subflorescence, which is usually a fraction of a millimetre to a

D. Benavente
Laboratorio de Petrología Aplicada. Unidad Asociada CSIC-UA. Dpto. Ciencias de la Tierra y del Medio Ambiente, Universidad de Alicante, 03080 Alicante, Spain; e-mail: david.benavente@ua.es

L. Linares-Fernández
Dpto. de Construcciones Arquitectónicas, Universidad de Alicante, 03080 Alicante, Spain

G. Cultrone · E. Sebastián
Dpto. de Mineralogía y Petrología, F. de Ciencias, Universidad de Granada, Fuentenueva s/n, 18002 Granada, Spain

few millimetres from the surface and produces outward blistering and peeling which in turn flakes off or powders away [3, 4].

The damage that may occur due to salt crystallisation is strongly influenced by both pore structure and strength properties. Pore structure has a great influence on salt crystallisation, including nucleation and precipitation, capillary rise of solutions, evaporation of water and the effects of the wetting and drying cycles.

The main pore structure parameters that affect brick durability are porosity, pore size distribution and pore shape.

Porosity, P, is defined as the ratio of the volume of voids to total volume of brick, expressed as a percentage. More specifically, connected porosity is related to the flow of weathering agents and the remaining moisture in such a way that it produces a negative influence on brick durability.

Different theoretical approaches have shown that salt damage processes, such as salt crystallization [2] or thermal expansion of salts [5, 6], depend greatly on pore structure parameters. Moreover, it has been demonstrated through experiments that porous bricks with a high porosity and a large percentage of pores measuring less than 1–2.5 μm in radius, are most prone to decay [7–9]. This is due to the fact that several important decay mechanisms are inversely related to pore size, such as frost and salt action as well as capillary pressure during the wetting and drying cycles [1, 6].

For example, Maage [7] investigated the relationship between pore size distribution and pore volume as regards the frost retention of the brick. He proposed an equation that allows a brick's durability factor to be calculated from connected porosity, P_V, and the percentage of pores which are larger than 3 μm in diameter, P_3, as follows:

$$DF = \frac{3.2}{Pv} + 2.4 \cdot P_3 \tag{1}$$

As salt and ice growth within porous materials has a similar mechanical action [1, 2, 6], Maage's equation may be used in order to estimate brick durability under the effects of salt crystallisation.

On the other hand, Ordóñez et al. [10] have estimated stone durability based on the fact that crystallisation pressure is inversely related to pore size, extrapolating salt stress in one pore to the whole porous stone. This fact was described by defining the durability dimensional estimator (*DDE*) as follows:

$$DDE(\mu m^{-1}) = \sum \frac{D_v(r_i)}{r_i} P_{conc} \tag{2}$$

where D_v is the pore size distribution, r_i is the pore size, and P_{conc} is the connected porosity.

Pore shape is closely related to brick durability as it affects salt nucleation, the flow of fluids and the condensation-evaporation process. There are several parameters that describe pore shape including the well-established fractal theory, in which the fractal dimension, FD, quantifies the pore shape or the pore surface roughness [11]. The pore shape can also be derived from the circularity of the cross-section of the hydraulic radius of the pore that controls the flow properties [12].

Capillary transport is an important flow mechanism as regards brick durability since it is closely related to the transportation of ions through the porous material, to the evaporation process and to the wetting and drying cycles [13]. This flow mechanism can be quantified by the water absorption coefficient, C, which is very much linked to the characteristics of both the pore structure and the fluid [14–16].

The susceptibility of the brick to the salt crystallisation mechanism is also closely connected to strength which is the material's resistance to crystallisation pressure. For example, in bricks with a high compression strength, Young's module or ultrasonic wave propagation velocities tend to have a longer durability [17]. Benavente et al. [18] defined a petrophysical durability estimator, *PDE*, which takes into account both pore structure and rock strength and represents the relationship between crystallisation pressure and material resistance. From this study, it is concluded that durability of porous materials can be estimated by the relationship between *DDE*, which provides full information about pore structure and tensile strength, due to the fact that the crystallisation pressure of salt creates tensile stress over the pore surface.

Brick is a traditional building material, known to have been used in constructions since before 1530 B.C. in Egypt [19]. The term "brick" encompasses a wide number of products obtained by mixing, preparing and moulding clay, slow drying and, finally, firing it in appropriate ovens. During the firing process, liquid water and structural water are driven off. As the temperature rises, mineralogical and textural changes occur. These are the results of the marked imbalance of a system that, to a certain degree, resembles high-temperature metamorphic processes (e.g., contact aureoles in pyrometamorphism). Under these conditions, rapid heating triggers the mineral reaction, preventing the formation of stable phases and favouring less stable ones (e.g., mullite, gehlenite; [20]). Porosity is directly related to the mineralogical composition of the raw material, since ceramics manufactured with a high sand fraction tend to be extremely porous and permeable [21]. Products fired at high temperatures are generally more vitreous, have a higher degree of durability and undergo the greatest changes in pore size and porosity [9, 22, 23]. Thus, the composition of the original clay combined with the production process, particularly the firing temperature, all

determine the quality of the final product and, therefore, its susceptibility to the salt crystallisation mechanism [24].

The aim of this paper is to evaluate the variation of brick's susceptibility to the salt crystallisation mechanism produced by the microstructure modification during firing, and, consequently, to determine the best firing temperature to increase its durability.

2. Materials and methods

2.1. Material studied

Solid bricks were prepared by hand in the laboratory. 400 ml water was added to each kg of raw material to make the clay plastic. The clay was then placed in a wooden mould ($24.5 \times 11.5 \times 4$ cm) to shape the bricks, which were subsequently air-dried. The average temperature and relative humidity in the laboratory were 25°C and 50%, respectively. The raw material is predominantly siliceous and presents a high concentration of phyllosilicates (i.e., clay minerals). Even if only one clayey material is considered in this investigation which can limit the generality of the findings, it can be considered to be representative of the main types of raw clay materials commonly used in the brick-making industry [25,26].

The samples were fired in an electric oven (Herotec CR-35) at a temperature, T, of: 700°C (G7), 800°C (G8), 900°C (G9), 1000°C (G10) and 1100°C (G11). The T was kept at 100°C for one hour and then at the maximum T for three hours. The heat was increased by approximately 3°C per minute.

The firing T determined the development of new mineral phases in the bricks. According to previously published studies, the mineralogical and textural results of these bricks can be summarised as follows [20]: It can be said that all phyllosilicates disappeared except the dehydrated phase of the illite, whose concentration dropped as the T increased and disappeared at T greater than 900°C. The microcline structure collapsed and/or partially transformed into sanidine. Mullite + sandine developed in such a way that the muscovite and/or illite disappeared at $T \geq 800$°C. The mullite, formed by the epitactic replacement of muscovite, followed the orientation of the mica crystals. This latter reaction was favoured by the lesser amount of free energy needed during the transition phase [27]. The content of non-crystalline phases increased as the firing T grew, especially at high T [28].

From a textural point of view, at a low firing T, the laminar habit of the phyllosilicates was distinguished although the muscovite appeared with a marked exfoliation along its basal planes, due to dehydration. The interconnection among particles was limited and there was no evidence of vitrification or sintering. At 900°C, the pores maintained an irregular shape and angular borders whilst the phyllosilicates became deformed and coalesced with each other. The partial vitrification of mineral grains was significant at 1000°C when the pores adopted an ellipsoidal shape and smooth borders. At 1100°C, vitrification was complete. The pores coalesced forming spherical-shaped cells, as a consequence of the melting of the clay particles and the expansion of gases trapped within the raw materials [29], generating the so-called "cellular structure" [30]. The evolution of the textural characteristics is shown in Fig. 1.

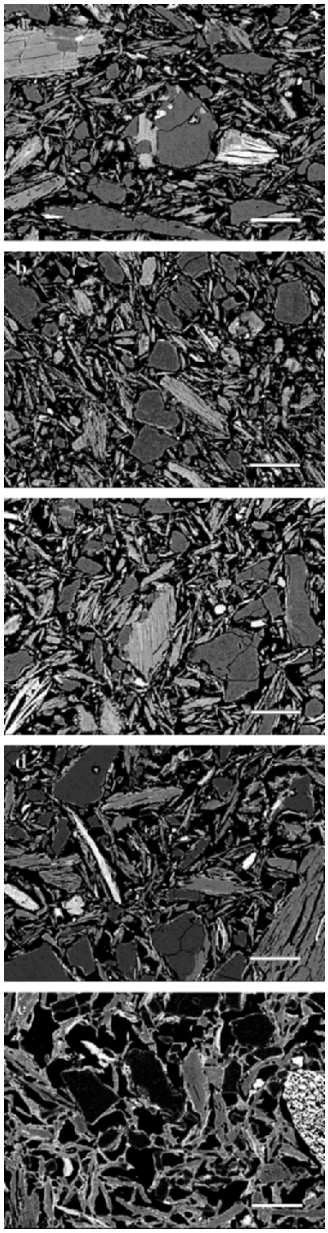

Fig. 1 Backscattered electron images of bricks fired at: (a) 700, (b) 800, (c) 900, (d) 1000 and (e) 1100°C. The white bar indicates 50 μm.

Table 1 Porosity, P; mean radius, r; roundness, δ; fractal dimension; FD; water absorption coefficient, C; and percentage of dry weight loss of bricks at different firing temperatures

Parameter	G7	G8	G9	G10	G11
T [°C]	700	800	900	1000	1100
P [%]	38.63	39.28	37.41	27.49	19.45
r [μm]	0.57	0.63	0.72	1.37	1.67
δ	0.16	0.16	0.16	0.20	0.39
FD	1.64	1.60	1.58	1.51	1.31
C [g/(cm^{2}min$^{0.5}$)]	3.30	3.19	3.05	2.50	1.84
σ_C [MPa]	3.31	2.24	9.00	15.33	21.82
v_P [km/s]	1.03	1.14	1.55	2.00	2.42
DWL [%]	9.18	0.75	0.20	0.00	0.00

2.2. Porous media characterization

In order to characterise the evolution of the porous media of the bricks in terms of firing T, the mercury intrusion porosimetry (MIP) technique, digital image analysis of SEM backscattered electron images (BSEI) and capillary imbibition tests were used.

MIP is an extensively used porous media characterisation technique. Connected porosity, pore size distribution and mean pore size were obtained using a Micromeritics AutoPore III 9410 porosimeter, which can exert a maximum injection pressure of 414 MPa. Brick samples (~2 cm^3) were collected before and after the salt crystallisation test and dried (at 110°C, 24 hours) prior to MIP analysis. Two measurements were taken per brick (*Table I*, Fig. 2).

In order to calculate both fractal dimension and pore roundness, BSEI were carried out. A JEOL JSM-840 and polished thin sections of brick samples were used. The fractal dimension, obtained from back scattering electron image (BSEI) analysis, is calculated as follows [11]:

$$P = \varepsilon^{FD} A^{FD}/2, \tag{3}$$

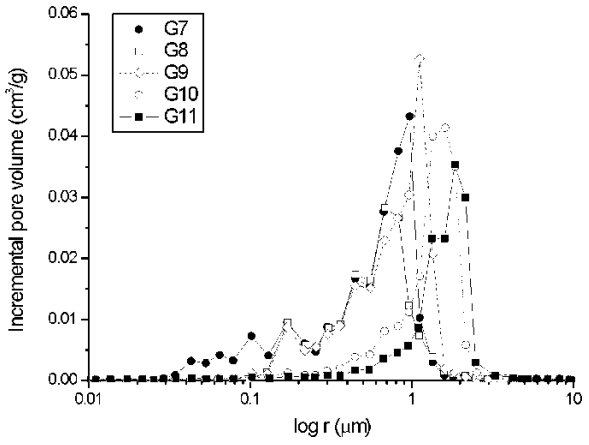

Fig. 2 Evolution of pore size distribution of bricks at different firing temperatures.

where P and A are the pore perimeter and area respectively, ε is a constant that depends on the length of the measuring grid size, and FD is the fractal dimension. Thus, the fractal dimension is easily achieved from the slope of the log A – log P plot. The Euclidian dimension for a line and an area is, respectively, 1 and 2, and is always exceeded by the fractal dimension. Therefore, the implication of a fractal dimension between 1 and 2 is that the pore perimeter is irregular and tends to fill the pore area as FD increases.

The pore roundness, δ, used in this study is based on flow properties and defined as follows:

$$\delta = \frac{4\pi A}{P^2}, \tag{4}$$

This pore shape, which is dimensionless and orientation–independent, has a maximum value of unit per circle and progressively decreases as it loses its circular form.

Both fractal dimension and pore roundness were calculated studying SEM images at a magnification of 400× (*Table I*). This intermediate magnification was chosen as lower magnifications would give a poor resolution whilst a higher magnification would considerably reduce the size of the field observed, possibly hindering pore shape measurements. Image analysis was performed using the UTHESCA ImageTool® [31].

The capillary imbibition test is widely used for the characterisation of building materials and provides information about their pore structure and durability. Three parallelepiped-shaped (7 × 3.5 × 2 cm) samples were used per brick and the test was performed according to NORMAL 29/88 [32]. The results were plotted as absorbed water per area of the sample throughout imbibition versus square root of time. With this kind of representation, the capillary imbibition kinetic shows two parts: the first, which defines water absorption, and the second, which defines saturation. The slope of the curve during water absorption is the water absorption coefficient, C (*Table I*). This parameter is essentially equivalent to the sorptivity parameter in soil physics [33].

2.3. Mechanical properties

Ultrasonic wave propagation was selected to monitor the porosity evolution of brick samples fired at different T. The ultrasonic longitudinal waves, v_p, were measured in three directions perpendicular to each other. v_P values were obtained using an ultrasonic generator Steinkamp BP-5, with 100 kHz transducers (*Table I*).

In order to corroborate these results, 3 cube-shaped samples (measuring 3 cm along each side) were subjected to uniaxial unconfined compression resistance (σ_C) for each T, exerting pressure perpendicular to the layering of the bricks,

according to the ASTM D 2938 regulation [34]. This test was performed using a Metro Com MI 30 press with a 3×10^5 kg load capacity (*Table I*).

2.4. Salt crystallisation

Parallelepipedic bricks ($7 \times 3.5 \times 2$ cm) were used for the salt crystallisation test. Bricks were weighed before the test to check salt damage and were placed vertically into cylindrical glass beakers (115 mm diameter and 65 mm high). Brick samples were partially immersed in a Na_2SO_4 saturated solution, which was covered with melted paraffin to avoid evaporation and to let the solution flow through the capillary pore system. No relative humidity or temperature variation occurred during the experiment and, consequently, only continuous evaporation, supersaturation and salt crystallisation were produced. Neither deliquescence of the existing salts followed by reprecipitation nor any hydration process take place under such conditions. Therefore, a single damage process was brought about solely as a result of crystallisation pressure [4].

After this, the tested samples were cleaned with deionised water until all remaining salt was removed. The samples were dried (60°C) until they reached a constant weight. The dry weight loss (*DWL*) was calculated at this stage (*Table I*).

3. Results and discussion

3.1. Evolution of pore structure

The influence of firing *T* on the evolution pore structure parameters (porosity, mean radius, roughness, fractal dimension and water absorption coefficient) are quantified in *Table I*. The evolution of pore structure can be explained by the mineralogical and textural changes during the firing of clays. Thus, at lower *T*, pores are spread out and more distributed, although a preferred orientation of elongated pores is observed, due to the disposition of the phyllosilicates. At 1000 and 1100°C, pores become larger and rounder, the so-called "cellular structure". The smaller pores tend to disappear as the larger ones increase and take over (Fig. 1).

Generally speaking, porosity decreases whilst pore radius increases and as the firing *T* increases (Fig. 2). On the other hand, pores tend to become rounder. This fact can be observed in the evolution of both fractal dimension and roundness (Table I). The fact that fractal dimension tends to one, as firing *T* increases, implies that the pore perimeter is regular. Roundness was defined as the ratio between the hydraulic radius with a non-circular cross-section and a circular cross-section (Eq. (4)). As a result, this pore shape progressively increases to a maximum value of unit as it achieves its circular form.

It can also be observed that the hydric behaviour of bricks varied with the firing *T* (*Table I*). This can be explained by the strong influence that pore structure has on the water absorption coefficient, *C*, which may be expressed by:

$$C = P\rho\sqrt{\frac{r\delta\gamma\cos\theta}{2\tau\eta}}, \tag{5}$$

where *P* is the porosity, r the effective radius, τ the tortuosity, δ the roundness, ρ the density of the fluid, γ is the interfacial tension of the fluid, θ the contact angle and η is the viscosity of the fluid [16]. Thus, at 700 and 800°C pore radius and roundness have a strong influence on this coefficient, whereas, at 1100°C the most important parameter is porosity. However, between 900 and 1000°C the evolution of the whole porous media parameters is reflected in the water absorption coefficients. As a result, solid bricks with thin pores present a small water absorption coefficient value and, consequently, this is inversely related to brick durability.

3.2. Mechanical properties of bricks

It has been found that ultrasound velocity v_P increases as the firing *T* increases. This is a consequence of the vitrification of the bricks as the *T* rises in accordance with SEM observations. This change in texture generates a more homogeneous brick, including a reduction of weak planes. The uniaxial compression test offers similar results to the ultrasound (*Table I*). Both tests revealed minimal changes between 700 and 800°C and no changes in the texture of bricks were observed. However at temperatures of above 800°C, there is a constant increase in ultrasonic wave velocity and compression resistance values.

3.3. Brick susceptibility to salt crystallisation

Salt decay by Na_2SO_4 crystal growth is shown in Fig. 3. Thus, Na_2SO_4 crystallises within brick pores, as subflorescence, at a few millimetres beneath the external surface. This mechanical action generates enough crystallisation pressure to cause outward peeling and granular disintegration. Finally, where the wall is dried, whiskers tend to form, as ions only reach the base of the crystal as it grows away from the surface. This kind of efflorescence is mainly produced in G7, G8 and G9, where vitrification is scarcer.

Salt crystallisation action and, therefore, brick durability, have been quantified using the percentage of weight loss after salt crystallisation, *DWL* (*Table I*). Brick durability is firstly influenced by both pore structure and material strength and increasing the firing T results in greater mechanical strength (ultrasound velocity and uniaxial compressive strength), lower porosity, bigger and rounder pores. All these

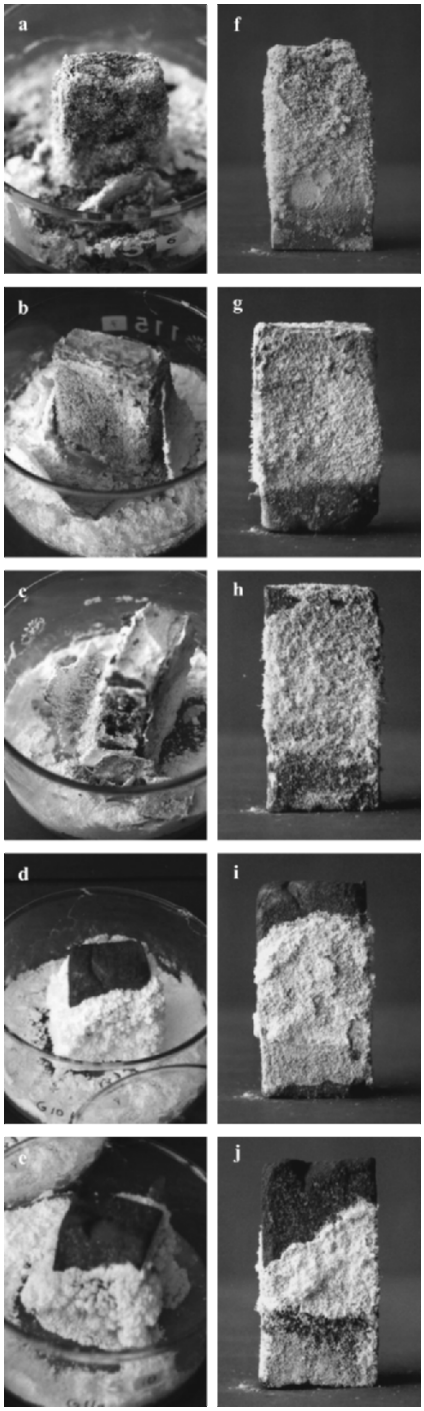

Fig. 3 The visual appearance after salt crystallisation test of bricks fired at: (a,f) 700; (b,g) 800; (c,h) 900; (d,i) 1000 and (e,j) 1100°C.

factors should increase brick durability and, more specifically, its resistance to salt crystallisation.

As crystallisation pressure produces mechanical stress on pore surfaces, brick strength therefore plays an essential role in resistance to decay. It can be said that a brick with excellent mechanical properties is less prone to decay as a result of salt crystallisation [17]. This assertion can be deduced by comparing the increase in compression strength and ultrasonic velocities with the decrease in weight loss as the firing T rises (*Table I*).

The evolution of the studied bricks' susceptibility to decay is also observed in the durability estimators (Table 2). On the one hand, porous materials with high porosity and thin pores are more prone to decay [2, 7–9, 35,36] and, therefore, low *DF* values and high *DDE* values lead to lower brick durability. G7, G8 and G9 have a pore radius smaller than 1 μm and are thus more prone to decay than G10 and G11, with a pore radius greater than 1 μm. Moreover, the porosity of G7, G8 and G9 (38.63, 39.28 and 37.41%, respectively) is larger than in the G10 and G11 bricks (27.49 and 19.45%, respectively).

On the other hand, small *PDE* values indicate a greater brick durability as crystallisation pressure is less than the resistance to salt stress. Salt crystallisation (and other decay mechanisms) is closely related to pore size and porosity. As we have previously mentioned, increasing the firing *T* results in lower porosity and larger pores in such a way that brick susceptibility to crystallisation pressure decreases. Furthermore, mechanical strength increases as the firing *T* rises and, consequently, the resistance of the brick to salt stress increases considerably. Therefore, the evolution of both pore structure and brick strength explains the excellent durability of G10 and G11.

4. Concluding remarks

In this study, the importance of both pore structure and strength on brick durability has been highlighted. A relationship has been observed between the effectiveness of salt crystallisation and the resistance of bricks to salt stress. An increase in the firing temperature produces a more homogeneous and resistant brick, measured using ultrasound velocity and uniaxial compressive strength. This result is obtained thanks to the vitrification process and changes in the brick's pore structure: larger, rounder pores, which are quantified by their roundness and fractal dimension.

Improving the resistance of bricks to the salt crystallisation mechanism is an important task since this kind of construction material is often used in the restoration of historic buildings and also such a decay process is not only aggressive but also common. Bricks fired at temperatures above 1000°C give the best results in the parameters used to determine quality. Therefore, it is advisable to apply such firing temperatures when the raw material used has a similar mineralogical composition and production process to those studied here. Considering that few differences are noted in pore structure and brick strength between 1000 and 1100°C, the recommended firing temperature is 1000°C, as this involves a lower production cost than firing at 1100°C.

Table 2 Durability factor, DF; durability dimensional estimator, DDE; petrophysical durabilty estimator, with respect to uniaxial compressive strength, PDE_C; and ultrasonic velocity, PDE_{Vp}, of bricks

Estimator	G7	G8	G9	G10	G11
DF	24.47	33.76	23.93	122.60	167.32
DDE [μm^{-1}]	0.92	0.55	0.42	0.24	0.23
PDE_C (1)	0.27	0.24	0.05	0.02	0.01
PDE_{Vp} (2)	8.91	4.85	2.72	1.20	0.54

(1) $PDE_C = 10^{\frac{DDE}{\sigma_C}}$ (2) $PDE_{Vp} = 10^{\frac{DDE}{V_P}}$

Acknowledgements This work was supported by the Research Project MAT2004-6804, and the Research Groups RNM179 of the Junta de Andalucía and 03/158 of Comunidad Valenciana.

References

1. Winkler EM (1997) Stone in architecture: Properties, durability. 3rd edn, Springer-Verlag, Berlin.
2. Scherer GW (1999) Crystallization in pores. Cem. Concr. Res. 29:1347–1358.
3. Lewin SZ (1981) The mechanism of masonry decay through crystallisation. Conservation of Historic Stone Building and Monuments, National Academy of Sciences, Washington DC, 120–144.
4. Rodríguez-Navarro C, Doehne E (1999) Salt weathering: Influence of evaporation rate, supersaturation and crystallisation pattern. Earth Surf. Process. Landforms 24:191–209.
5. Larsen ES, Nielsen CB (1990) Decay of bricks due to salt. Mater. Struct. 23:16–25.
6. Scherer GW, Flatt RJ, Wheeler G (2001) Materials science research for the conservation of sculpture and monuments. MRS Bull. 26:44–50.
7. Maage M (1980) Frost resistance and pore size distribution in bricks. Report No. RM1 80-201, Norwegian Inst. of Techn., Univ. of Trondheim, Trondheim.
8. Robinson GC (1984) The relationship between pore structure and durability of brick. Am. Ceram. Soc. Bull. 63:295–300.
9. Winslow N, Kilgour CL, Crooks RW (1988) Predicting the durability of bricks. J. Test. Eval. 16:527–531.
10. Ordóñez S, Fort R, García del Cura MA (1997) Pore size distribution and the durability of a porous limestone. Q. J. Eng. Geol. 30:221–230.
11. Mandelbrot BB (1982) The fractal geometry of nature. W. H. Freeman, S. Francisco.
12. White FM (1991) Viscous fluid flow. 2nd edn, McGraw-Hill, New York.
13. Scherer GW (2004) Stress from crystallization of salt. Cem. Concr. Res 34:1613–1624.
14. Dullien FAL, El-Sayed MS, Batra VK (1977) Rate of capillary rise in porous media with nonuniform pores. J. Colloid Interf. Sci. 60:497–506.
15. Hammecker C, Jeannette D (1994) Modelling the capillary imbibition kinectics in sedimentary rocks: Role of petrographical features. Transport in Porous Med. 17:285–303.
16. Benavente D, Lock P, García del Cura MA, Ordóñez S (2002) Predicting the capillary imbibition of porous rocks from microstructure. Transport in Porous Med. 49:59–76.
17. Elert K, Cultrone G, Rodríguez-Navarro C, Sebastián E (2003) Durability of bricks used in the conservation of historic buildings—Influence of composition and microstructure. J. Cult. Herit. 4:91–99.
18. Benavente D, García del Cura MA, Fort R, Ordóñez S (2004) Durability estimation of porous building stones from pore structure and strength. Eng. Geol. 74:113–127.
19. de Buergo Ballester MA, González Limón T (1994) Restauración de edificios monumentales. Monografías del Ministerio de Obras Públicas, Transportes y Medio Ambiente.
20. Cultrone G, Rodríguez-Navarro C, Sebastián E, Cazalla O, de la Torre MJ (2001) Carbonate and silicate phase reactions during ceramic firing. Eur. J. Mineral. 13:621–634.
21. Warren J (1999) Conservation of brick. Butterworth Heinemann, Oxford.
22. Delbrouck O, Janssen J, Ottenburgs R, Van Oyen P, Viaene W (1993) Evolution of porosity in extruded stoneware as a function of firing temperature. Appl. Clay Sci. 7:187–192.
23. Cultrone G, Sebastián E, Elert K, de la Torre MJ, Cazalla O, Rodríguez-Navarro C (2004) Influence of mineralogy and firing temperature on porosity of bricks. J. Eur. Ceram. Soc. 24:547–564.
24. Binda L, Baronio G (1984) Measurement of the resistance to deterioration of old and new bricks by means of accelerated aging tests. Durability of Building Materials 2:139–154.
25. Dondi M, Ercolani G, Fabbri B, Marsigli M (1998) An approach to the chemistry of pyroxenes formed during the firing of Ca-rich silicate ceramics. Clay Miner. 33:443–452.
26. Riccardi MP, Messiga B, Duminuco P (1999) An approach to the dynamics of clay firing. Appl. Clay Sci. 15:393–409.
27. Rodríguez-Navarro C, Cultrone G, Sánchez-Navas A, Sebastián E (2003) Dynamics of high-T muscovite to mullite transformation: A TEM study. Am. Mineral. 88:713–724.
28. Cultrone G (2001) Estudio Mineralógico-petrográfico y físico-mecánico de ladrillos macizos para su aplicación en intervenciones del Patrimonio Histórico. PhD Thesis. Universidad de Granada, Granada.
29. Parras J, Sánchez Jiménez C, Rodas M, Luque FJ (1996) Ceramic applications of middle Ordovician shales from central Spain. Appl. Clay Sci. 11:25–41.
30. Tite MS, Maniatis Y (1975) Examination of ancient pottery using the scanning electron microscope. *Nature* 257:122–123.
31. UTHESCA ImageTool®. Develop at the University of Texas Health Science Center at San Antonio (Texas, 1995), http://www.from maxrad6.uthesca.edu.
32. NORMAL 29/88, Misura dell'indice di asciugamento (drying index). CNR-ICR, Roma, 1988.
33. Zimmerman RW, Bodvarsson G (1991) A simple approximate solution for horizontal infiltration in a Brooks-Corey medium. Transport in Porous Med. 6:195–205.
34. ASTM D 2938 (1986) Standard test method for unconfined compressive strength of intact core specimens.
35. Wellman HW, Wilson AT (1965) Salt weathering, a neglected geological erosive agent in coastal and arid environments. Nature 205:1097–1098.
36. La Iglesia A, González V, López-Acevedo V, Viedma C (1997) Salt crystallization in porous construction materials I. Estimation of crystallization pressure. J. Cryst. Growth 177:111–118.